WARSAW UNIVERSITY OF TECHNOLOGY Index 351733
FACULTY OF CIVIL ENGINEERING
COMMITTEE FOR CIVIL AND WATER ENGINEERING
POLISH ACADEMY OF SCIENCES ISSN 1230-2945

DOI: 10.24425/ace.2021.138074

ARCHIVES OF CIVIL ENGINEERING

Vol. LXVII ISSUE 3 2021

s. 619–638

Research Paper

Analysis of the structural response of Beirut port concrete silos under blast loading

S.A. Ismail[1], W. Raphael[2], E. Durand[3], F. Kaddah[4], F Geara[5]

Abstract: Several months after August 4, 2020, Lebanon is still recovering from the enormous explosion at the port of Beirut that killed more than 200 people and injured more than 7500. This explosion ripped the city to shreds and significantly damaged the Beirut port silos. Saint Joseph University of Beirut "the school of engineering ESIB" in collaboration with "Amann" Engineering performed a 3D scan of the Beirut port silos to assess the silos' level of damage. The obtained data was then compared to the numerical modelling results, obtained from Abaqus explicit, in order to estimate the blast magnitude and to check if the pile foundation can be reused in building new silos at the same place due to the limited space available at the port of Beirut while considering the soil-foundation-structure interaction effect. In addition, the silos' structural response against the filling of the silos at the time of explosion was investigated. The displacement of the silos and the amount of silos' damage obtained from the fixed and flexible numerical models indicate that a blast magnitude of 0.44 kt TNT (approximately 1100 tons of Ammonium Nitrate) best estimates the 20 to 30 cm silos' tilting in the direction of the blast. In addition, the soil and the foundation played a positive role by absorbing part while dissipating less amount of the blast energy. Also, the grains at the time of the event did not affect the silos' deformation and damage amount. Noting that the displacement of the pile foundation exceeded all limits set by design codes, indicating that the pile foundation cannot be reused to build new silos at the same place.

Keywords: Blast Loading, Concrete failure, Finite element analysis, Soil-Structure-Foundation Interaction

[1] Phd, Civil Engineering Department, Saint Joseph University of Beirut, Beirut 17-5208, Lebanon, e-mail: sahar.ismail@net.usj.edu.lb, ORCID: https://orcid.org/0000-0003-2140-6969

[2] Professor, Civil Engineering Department, Saint Joseph University of Beirut, Beirut 17-5208, Lebanon, e-mail: wassim.raphael@usj.edu.lb,

[3] International expert, project support, Amann Engineering, Geneva 1212, Switzerland., Beirut 17-5208, Lebanon, e-mail: emmanuel@amann.engineering, ORCID: https://orcid.org/0000-0001-5134-5496

[4] Professor, Civil Engineering Department, Saint Joseph University of Beirut, Beirut 17-5208, Lebanon, e-mail: fouad.kaddah@usj.edu.lb, ORCID: https://orcid.org/0000-0003-0015-6390

[5] Professor, Civil Engineering Department, Saint Joseph University of Beirut, Beirut 17-5208, Lebanon, e-mail: fadi.geara@usj.edu.lb, ORCID: https://orcid.org/0000-0003-3829-1512

1. Introduction

On August 4, 2020, a devastating explosion at the port of Beirut struck the city and wounded more than 200 people, injured more than 7500 and caused more than $15 billion in damage (Fig. 1). The explosion created a crater of around 140 m wide, which was then flooded with seawater. It destructed structures several km away from the port and was heard as far away as Cyprus that is about 200 km across the Mediterranean Sea. This explosion, considered one of the most powerful explosions in history, was caused by fifteen tons of fireworks, several jugs of kerosene and acid in addition to thousands of tons of ammonium nitrate stored unsafely in the warehouse. These ingredients, combined, constructed the bomb that devasted the city [1, 2] and destructed the country's grain storage silos: the Beirut port silos.

Experts and researchers such as Bauer et al. [3] and King et al. [4] suggest that an uncontaminated Ammonium Nitrate cannot be easily detonated under normal conditions. In fact, Ammonium Nitrate's shock wave requires an enormous amount of energy. Blast incidents due to the explosion of Ammonium Nitrate go back to 1916. Since then, the chemical caused more than 30 disasters, some accidental and other intentional. Examples of these disasters are detailed in Table 1. Noting that the European's Seveso Directive [5], that regulates the storage and handling of all hazardous chemicals in Europe, lists Ammonium nitrate as a hazardous chemical.

Several researchers estimated the Beirut explosion blast magnitude using videos posted on social media, empirical formula, fireball analysis and geospatial data. Rigby et al. [6], using empirical formula, estimated the blast magnitude to an equivalent 0.55 to 1.1 kt of TNT. Diaz [7], using images and videos' recordings of the explosion that were posted on social media, estimated the blast magnitude to an equivalent 1.1 kt TNT. Also, Aaoud [8] using fireball analysis, estimated the blast magnitude to an equivalent 0.81 kt TNT. Stennett et al. [9] and Pasman et al. [10] used the videos posted on social media and analyzed the crater formed by the blast [10] to estimate the blast magnitude. They found that it is equivalent to 637 tons of TNT with a lower and upper bound of 407 and 1000 tons and 650 tons of TNT with a lower and upper bound of 300 and 1000 tons respectively. Also, Valsamos et al. [11] estimated the blast magnitude to an equivalent 1100 tons TNT using the geospatial data taken from the open source world map OpenStreetMap. On the other hand, USGS [12] estimated the size of the explosion to an equivalent M_w=3.3 magnitude earthquake.

Therefore, even though several features of seismic design of structures are recommended in blast design such as the ductile connections, some features may have opposite effects such as the decrease in the system's lateral resistance that can result in loss of the slab's capacity to transfer the

load to the column and thus, to the shear walls. As a result, researchers have been studying the responses of structures under seismic [13 to 16, etc.] and blast loadings [17 to 23, etc.]. Also, researchers have been analyzing the failure of real case studied structures [24 to 29, etc.]. Nevertheless, studies of silos subjected to external blast loadings are limited.

In this study, 3D scan of the Beirut port silos was compared to the 3D numerical modeling results to assess the level of damage of the silos and to estimate the blast magnitude. The numerical models were simulated using the finite element software Abaqus explicit and were based on the real silos' plans and project data. Moreover, the effect of the silos' structural response against the filling of the silos at the time of explosion was explored and assessed. As such, fixed and flexible-based models were hit by the blast loading and the silos' deformations in the direction of the explosion in addition to the amount of silos' damage and the effect of the soil-structure-foundation interaction (SSFI) were obtained. Whereas most of the research performed on the Beirut explosion is based on videos posted on social media, empirical formula, fireball analysis and geospatial data, the reality of the behavior is more complex. This study is the first to consider in addition to the concrete silos, the soil medium, the pile cap and the pile foundation. Therefore, the objective of this study was not only to estimate the blast magnitude, but also to investigate if the level of silos and piles deformations caused by the blast permits the pile foundation to be reused to build new silos at the same place due to the limited space available at the port of Beirut.

a)  b) 

Fig. 1. The Beirut port silos, a) before and b) after the August 4, 2020 blast [30, 31]

Table 1. Examples of worldwide accidents caused by Ammonium Nitrate and the corresponding charges

Blast incident location	Date	Casualties	Ammonium Nitrate (tons)
Texas, USA [32]	April 16, 1947	552 deaths	2086 & 870
Toulouse, France [33]	September 21, 2001	20 deaths	200–300
Mihailesti. Romania [34]	May 24, 2004	18 deaths	20
West Texas, USA [35]	April 17, 2013	15 deaths	240
Beirut port, Lebanon	Auhust 4, 2020	204 deaths	–

2. The Beirut port silos

In late 1960s, the largest grain storage facility at the time in the region: the Beirut port silos, started to be constructed. This project was constructed in three phases. Phase 1 of the project corresponded to 24 silos (8 columns × 3 rows of silos). Phase 2 corresponded to 18 silos (6 columns × 3 rows of silos), having the capacity of 105 000 tons of grains. Noting that phase 1 and 2 were completed in 1969. Finally, during phase 3 (in the 1990s), 6 extra silos (2 columns × 3 rows of silos) having the capacity of 15 000 tons of grains were added to fulfill the country's grains storage needs. The Beirut port outer silos, in 2000 to 2002, underwent restoration work due to concrete carbonation. In fact, the deterioration of these cells was mainly due to the exposure to humidity and salty seafront and thus, concrete carbonation. As detailed in Fig. 2, to reduce this damage, engineers reinforced these outer cells by jacking their inner walls by a 12 cm reinforced concrete coating. The internal wall thickness was increased from 17 to 20 cm and an extra layer of steel reinforcement was added. It should be noted that at the time of explosion, the silos were not filled completely with grains, as detailed in Fig. 3.

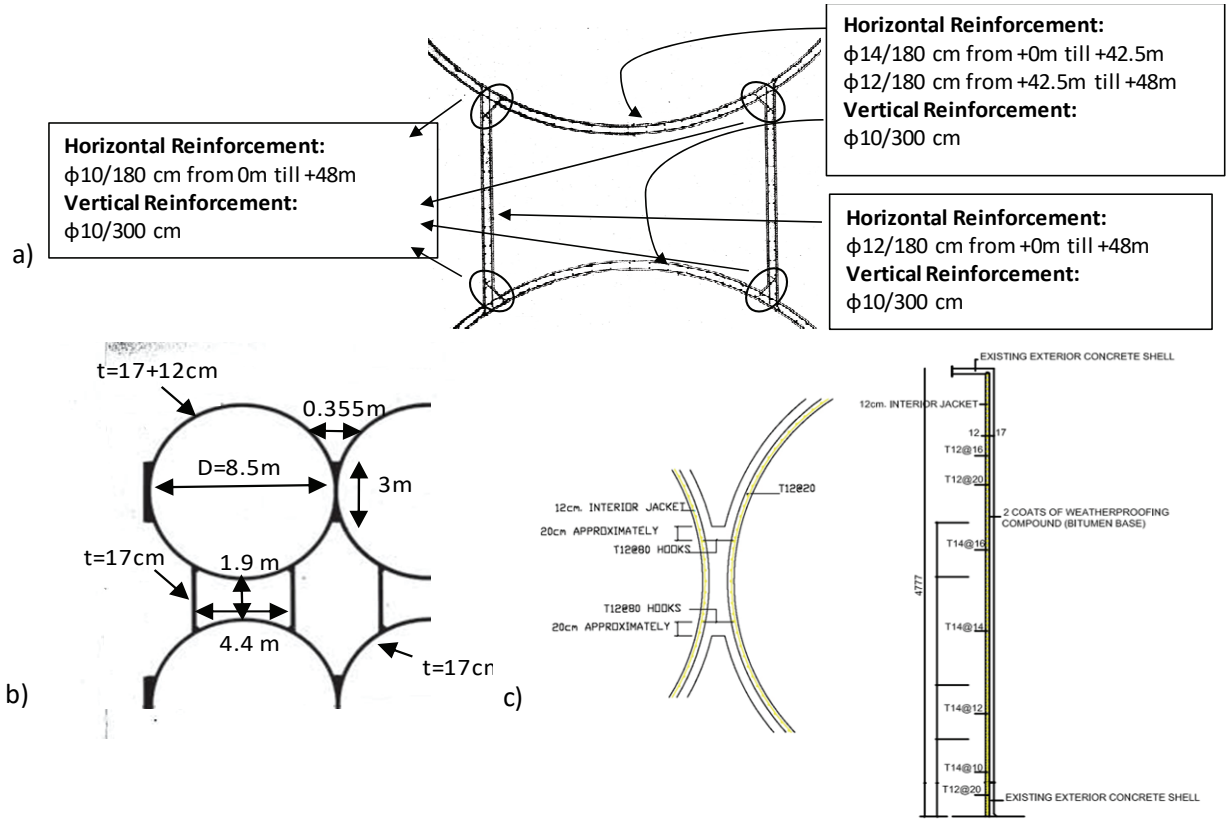

Fig. 2. a) The steel reinforcement; b) the geometry and c) the concrete and steel restoration work of the silos

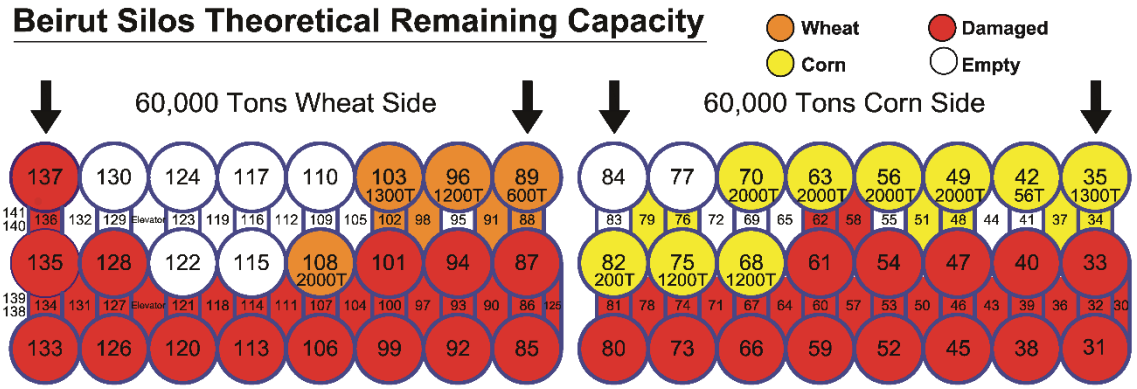

Fig. 3. Beirut silos grains capacity at the time of the blast

3. The 3D scan

Saint Joseph University of Beirut "the school of engineering ESIB" in collaboration with the swiss company "Amann" Engineering, performed a 3D scan to measure the damage in the Beirut port silos. This mission, executed in two phases, was performed after obtaining the permission of the investigation judge and the Lebanese army. 3D scan creates an exact copy of an object within minutes by taking and merging several snapshots of the object. 3D scan technology is being used in several industries such as engineering and medicine. It provides important data, accelerates the workflow, helps avoids expensive mistakes and enhances work productivity.

During the first phase in September 2020, the Swiss equipment LEICA BLK360 imaging scanner (Leica geosystems) was used. This equipment allows the acquisition of 3D points with integrated spherical imaging and thermography panorama sensor system in up to 360 000 points per second. LEICA BLK360 provides live image and scanner data stream viewing and editing with automatic tilt measurements. It completes a full dome scan, spherical and thermal 3D images with 6 mm at 10 m and 8 mm at 20 m point accuracy in less than 3 minutes. It is based on high speed time of flight enhanced by Waveform Digitizing (WFD) distance measurement system technology. In addition, the camera system is formed of 15 Mpixel camera system, 150 Mpixel full dome capture, HDR, LED flash Calibrated 360° × 300° spherical image. While the thermal camera FLIR technology is based on longwave infrared camera with thermal 360° × 70° panoramic image. During the second phase in November 2020, the German equipment Z+F Imager 5010X scanner (Zoller & Fröhlich) was used. This equipment, that comes with a special navigation system, estimates the scanner position and orientation to support the Z+F Laser Control registration

software during pre and post registration on site. In addition, it includes a dynamic compensator that corrects angular tilts for each pixel during scan acquisition that has a rate of 1 million pixels per second. Z+F Imager 5010X scanner comes with an external thermal camera (Z+F T-Cam). This camera allows the application of infrared information to the scan. Thus, it generates 360° "full dome" thermal panorama scans in a fully automatic process. This equipment is widely used in the fields of insurance, architecture, facility management, cultural heritage, industry and forensics. This is because of its ability to record a full panorama (32 images) in 1:45 minutes with a resolution of 382 × 288 pixel and an infrared spectrum of 7.5 to 13 μm as well as a lens' field of view of 62° × 49°. As a result, the thermo-panorama is scaled to scan resolution of 2500 pixel at 360° with a working range greater than 1.6 m, a vertical field of view of 284° and a horizontal field of view of 360°. The 3D scan was performed using the LEICA BLK360 imaging scanner and Z+F Imager 5010X scanner for several reasons:

- The scope range: Using the LEICA BLK360 imaging scanner, and since the silos are 48 m height, the team had to stand far from the silos to capture the total silos' height and not be in danger. Whereas using the Z+F Imager 5010X, since it has a 3 times larger scope range than the LEICA BLK360, it swept a volume 27 times larger per scan in a smaller amount of time.
- The precision: Since it is a key parameter in surveying, the LEICA BLK360, due to its small size, was used in the slopes of the silos while walking on the grains. On the other hand, although the Z+F Imager 5010X provided more precise images, it was heavier and harder to manipulate than the LEICA BLK360.
- Number of points per second: This is a laser performance criterion. Although the LEICA BLK360 captured a decent amount of points per second, the Z+F Imager 5010X, adjusted the exposure time of each laser point which improved the measurements.
- Panoramic and thermal camera: The use of the Z+F Imager 5010X in the second phase allowed for a better final 3D scan result. This is since it is much more efficient in terms of color rendering as well as calibration between the laser device and the camera. It should be noted that the Z+F Imager 5010X is the only non-military scanner with a 3D high-resolution thermal camera.
- Dynamic compensation: This is related to the quality of the horizontal levelling. Even though the compensation is electronic and precise in LEICA BLK360, the compensation in Z+F Imager 5010X is not only electronic, it is also optional and mechanical with a higher precision level.

As a result, the level of damage of Beirut port silos was assessed by capturing 752 million points of measure in three dimensions using 25 stations in 360° panorama infrared images (Fig. 4). Due to August 4, 2020 blast, the first and second rows of silos were destroyed. The base of the first row of the silos is still visible, filled by wheat and corn (Fig. 1). However, the third row of silos, except the last two silos, remained intact. Nevertheless, the remaining standing silos exhibited some tilting. The 3D scan results, detailed in Fig. 5 and 6, show that, third row silos tilted at the head from 0 to 70 cm and at the bottom, they tilted from 0 to 55 cm with respect to the first silo. Therefore, they tilted between 20 and 30 cm in the direction of the blast. Fig 7 shows the 3D rendering of the silos that was executed by Bandara [36] who combined the 3D scan results with drone imaging conducted by the Lebanese ministry. Also, Fig. 8 presents the 3D scan executed by "ESIB" and "Amman" Engineering. The 3D scan indicates that, silos 4 and 5 exhibited the greatest amount of deformation/tilting without being destroyed while silos 15 and 16 were completely destroyed. The obtained deformations mean that the inner part of the silos is damaged, or the pile head is deformed beyond the elastic range or broken. To investigate if the level of silos and piles deformations caused by the blast permits the pile foundation to be reused to build new silos at the same place and to estimate the blast magnitude, 3D numerical models were simulated using Abaqus in the next section.

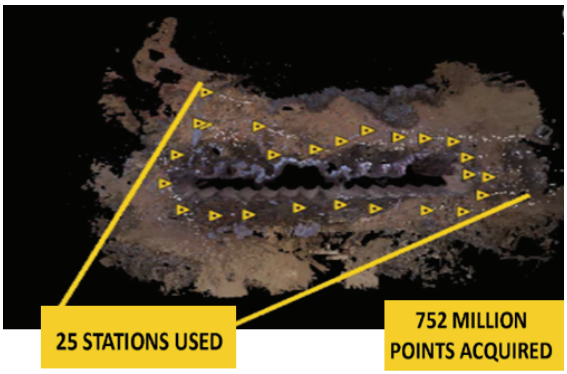

Fig. 4. The Beirut port silos 3D scan, points acquired, and stations used

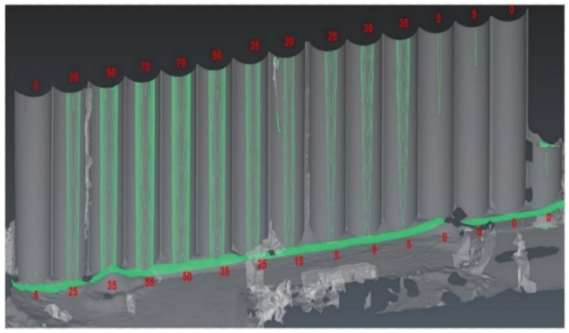

Fig. 5. The Beirut port silos deformation (in cm)-3D scan

Fig. 6. The Beirut port silos- processed image from drone-mounted LIDAR scan

Fig. 7. The Beirut Port Silos 3D scan [36]

Fig. 8 The Beirut Port Silos 3D scan (open the link to access the video)

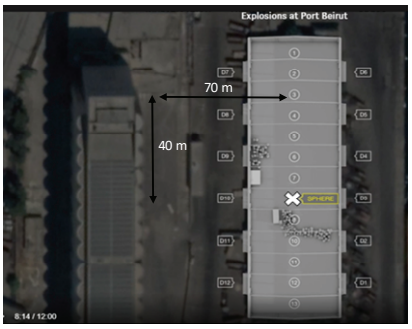

Fig. 9. The centre point of explosion

4. The numerical model

Fixed and flexible-based three-dimensional finite element models were built using Abaqus explicit [37] to simulate the blast of the Beirut port silos while considering the effect of soil- structure-foundation interaction effect (SSFI effect). This FE analysis uses an explicit integration solution technique to simulate brief dynamic events such as blast loading. In addition, it adopts a small increment size in the stiffness matrix which is updated at the end of each increment based on the geometry and the changes in the material. The 3D simulated models are based on the real plans and project data. As shown in Fig. 10, the numerical models were formed of the 8.5 m diameter, 48 m height reinforced concrete silos, the grains, the 140×30 m pile cap, the 2500 30×30 cm square driven 15 m length piles and the 460×200×17 m soil medium. The silos' geometry and steel reinforcement are detailed in Fig. 2. While the pile cap's thickness is equal to 3.12, 1.2 and 0.4 m between, at the edges and below the silos (Fig. 11). In addition, the first 2 m of the soil profile were defined as miscellaneous backfill sand material while the next 15 m were defined as sandy material that presents some levels of gravel and clay (Fig. 12). The silos, formed of 313 741 elements and the pile cap, formed of 7902 elements, were built using S4R shell elements while the grains, formed of 529 678 elements, were built using C3D8R solid elements. The silos and pile cap's steel reinforcements were defined as layers of reinforcement as part of the silos' and pile cap's shell elements using the rebars command available in Abaqus (rebars' layer option). The piles, formed of 17868 elements, were built using B31 beam elements and finally the soil medium, formed of 30400 elements, was built using C3D8R solid elements. To account for the absorbed energy from the unbounded soil domain, the far-field soil, in both horizontal directions, was modelled using 8-node linear one-way infinite brick elements CIN3D8. In addition, the bottom soil boundary was defined as a rigid boundary to simulate bedrock conditions.

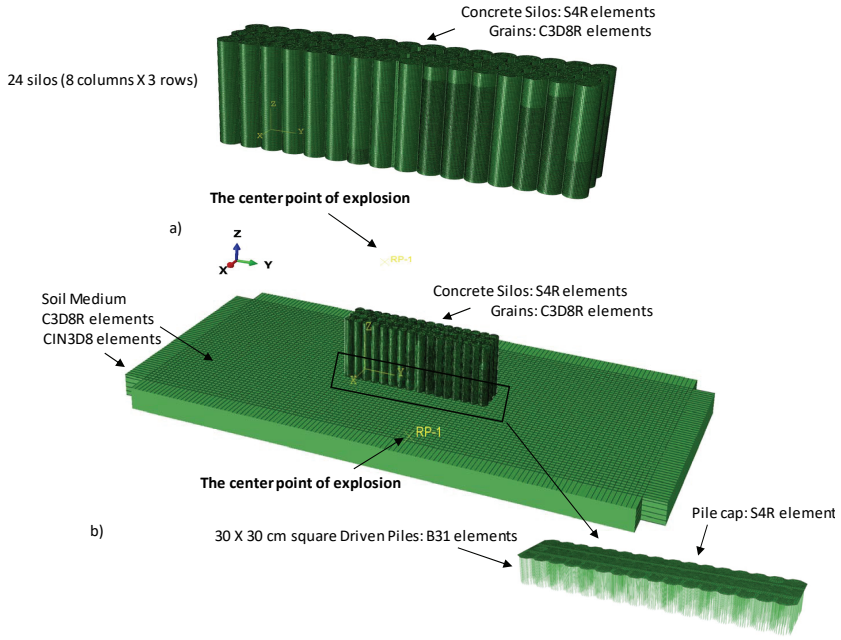

Fig. 10. a) Fixed-base and b) Flexible-base numerical models

In this study, the silos' concrete compressive strength f'_c was equal to 30 MPa. Moreover, the simplified damage plasticity model based on Hafezolghorani et al. [38] was used to define the concrete plasticity behavior of the silos while elastic-perfectly plastic material behavior was used to define the plasticity behavior of the steel reinforcement by defining the steel yield stress. Typical Mohr-Coulomb model was used to define the soil medium. Whereas, the grains: corn and wheat were assumed elastic based on EN1991-4 [39] provision. Noting that the grains were also simulated using plastic material. The results show that the permanent displacement at the head of the third row of silos slightly increases from elastic to plastic cases without affecting the amount of damage in the silos. For example, for the 0.3375 kt TNT case, the permanent displacement at the head of the third row of silos only increases by 2.18% from elastic to plastic cases (Fig. 13). Nevertheless, since the simulation running time of the plastic case needs twice as much as the elastic and the authors in this article wanted to account for the mass and movement of the grains, the grains were modelled using elastic properties. Table 2 shows the material properties adopted in the numerical model. In Table 2, ρ is density (kg/m^3), ν is the Poisson's ratio, σ_y is the yield stress (MPa), K is the ratio of the second stress invariant on the tensile meridian, fb0/fc0 is the ratio of initial equibiaxial compressive yield stress to initial uniaxial compressive yield stress, c is the soil cohesion (kPa) and Φ *and* ψ are the friction and dilation angles (°). In this study, the concrete and steel reinforcements in the silos and pile cap were tied using the tie command in ABAQUS. In addition, the silos and the pile cap as well as the pile cap and the piles' interface were modelled by tying the different parts together.

Table 2. Material properties

Steel Properties							
ρ (kg/m^3)		E (GPa)		v		σ_y (MPa)	
7850		206		0.3		448	
Wheat Properties				Corn Properties			
ρ (kg/m^3)		E (MPa)	v	ρ (kg/m^3)		E (MPa)	v
769		20	0.2	721		20	0.32
Concrete Properties							
ρ (kg/m^3)	v	ψ(°)	Eccentricity	*fb0/fc0*	K	Viscosity parameter	E (GPa)
2400	0.2	31	0.1	1.16	0.67	0	26.6
Backfill material							
ρ (kg/m^3)		E (GPa)		v	c (kPA)	Φ (°)	ψ (°)
1500		40		0.25	2	44	2.5
Sandy Soil with some levels of gravel and clay							
ρ (kg/m^3)		E (GPa)		v	c (kPA)	Φ (°)	ψ (°)
1700		25		0.25	10	38	10

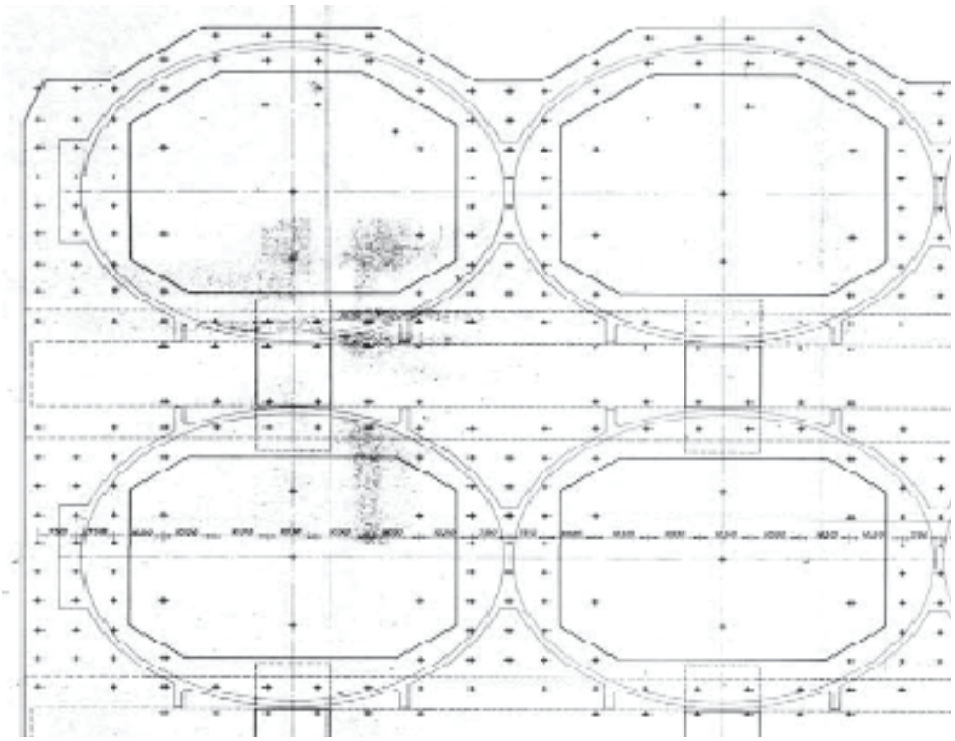

Fig. 11. The pile cap and driven piles' location

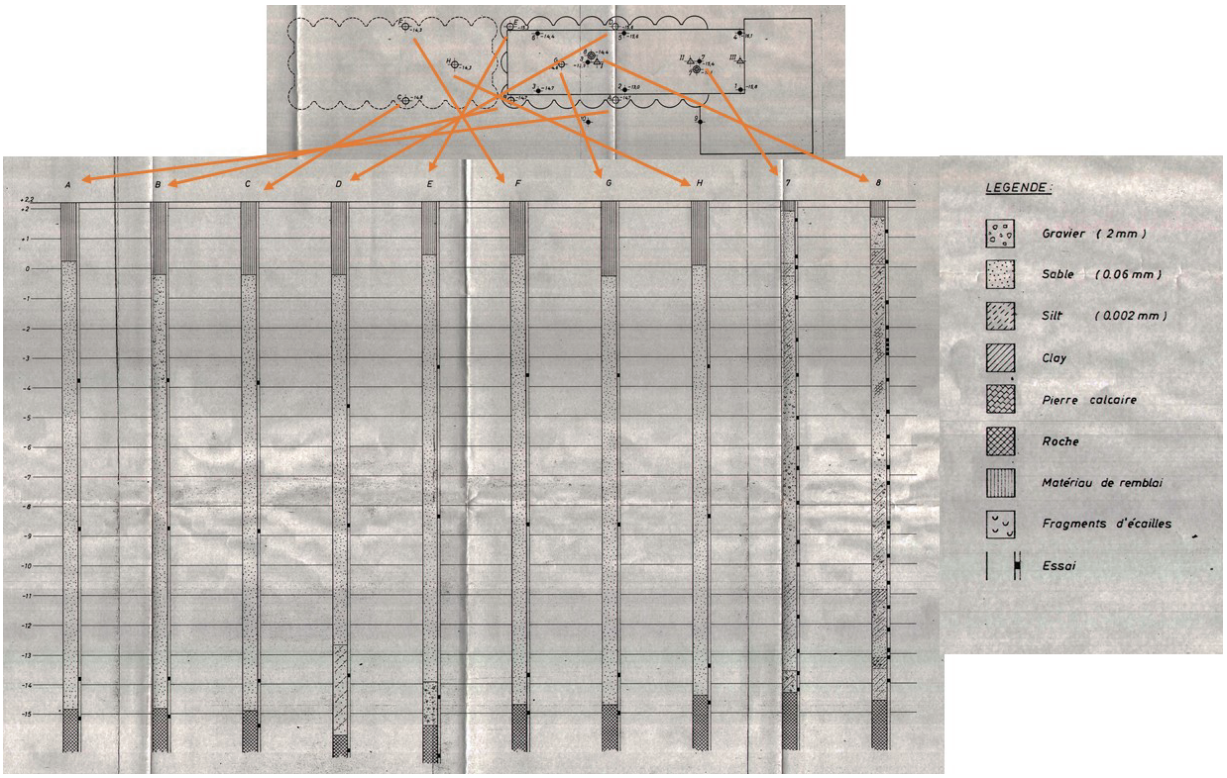

Fig. 12. Soil profile

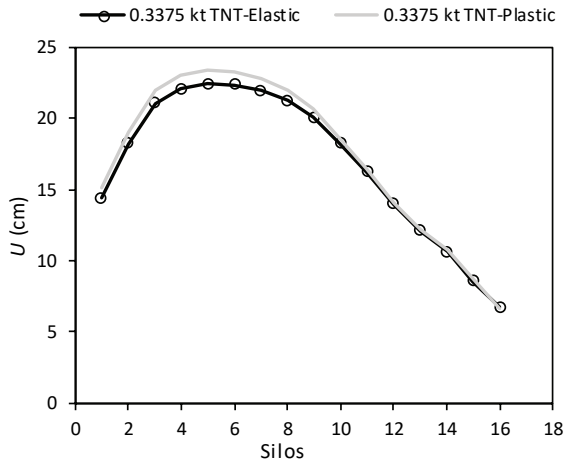

Fig. 13. Permanent displacement at the head of the third row of silos-0.3375 kt TNT elastic and plastic cases

The CONWEP method was used to simulate the blast loading that was applied at the silos' surface facing the explosion. This method allows the simulation of the loading effects due to explosion of a surface blast (hemispherical incident waves) in terms of both incident and reflected pressure. The center point of explosion was located at about 70 m in front of the silos and 40 m from the side of the silos in the warehouse which contained the explosive materials based on the Lebanese army aerial photos and the investigation report performed by Forensic Architecture [40] as detailed in

Fig. 9. Since CONWEP method requires the equivalent mass of explosive materials to be in terms of TNT, a scaling factor of 0.39 based on Krauthammer [41] study was used to convert the mass of Ammonium Nitrate into an equivalent mass of TNT based on the following equation:

$$W_{TNT} = W_{exp} X\ P_{exp}\ X\ \eta$$

where: W_{TNT} is the equivalent mass of TNT, W_{exp} is the weight of the explosive substance, P_{exp} is the explosive magnitude. It is defined by the ratio of the decomposition energy of 1 kg of substance (in J) divided by the detonation energy of 1 kg of TNT (J). And η is the efficiency of the explosion. It is defined by the ratio of the real emitted to the theoretical energy of the explosion [42].

5. Analysis of the different parameters' responses to blast loading

In this study, the blast magnitude was first estimated by comparing the 3D scan to the numerical modeling results. Then, the silos' structural response against the filling of the silos was analyzed.

5.1. Estimating the blast magnitude and the structural response

In order to check if the pile foundation can be reused to build a new silo at the same place, 3D scan results were first compared to the FE results to estimate the blast magnitude. Therefore, blast loadings of 0.375, 0.44, 0.55, and 1.1 kt (approximately 938, 1100, 1375 and 2750 tons of Ammonium Nitrate) were simulated. The blast loading was applied at the silos' surface facing the explosion with the explosion center point as detailed in Fig. 9. The displacement at the head and bottom of the silos in the direction of the explosion as well as the amount of silos' damage (degradation of the silos' elastic stiffness described by the compressive damage variable "d_c" (damage in compression) and the tensile damage variable "d_t" (damage in tension)) were extracted from the FE models. The damage variables range from 0: no damage to 1: destruction. Like the 3D scan results (Fig. 5), and as detailed in Fig. 14, that shows the displacements of the third row of silos in the direction of the explosion, the numerical results show that the first silo in the third row (the least damaged row), has lost its geometry and shape, the last two silos were completely destroyed while silos 4 and 5 exhibited the highest amount of displacement/tilting in the direction of the explosion without being destroyed. As such, silos 4 and 5 were considered as reference silos to estimate the blast magnitude and to perform the analysis.

Fig. 15 presents the displacements of the silos in the direction of the explosion for fixed and flexible-based models while Table 3 details the amount of displacements in silos 4 and 5 for the 3D scan and different numerical modeled cases. By comparing these results, we obtain that for flexible-based cases, the displacement increases from 60 to 93 cm at the head and from 30 to 44 cm at the bottom of silos 4 and 5 as the blast magnitude is increased from 0.3375 to 0.55 kt TNT. In addition, for fixed-based cases, the displacement increases from 23 to 38 cm at the head of silos 4 and 5 as the blast magnitude is increased from 0.3375 to 1.1 kt TNT. It should be noted that the 1.1 kt TNT case (approximately 2750 tons of Ammonium Nitrate) was only considered for a fixed-based scenario since it represents the total amount of Ammonium Nitrate it arrived at the port of Beirut in 2013. Therefore, since displacements of 70 and 53 cm were obtained at the head and bottom of silos 4 and 5 from the 3D scan, and 77 and 36 cm at the head and bottom of silos 4 and 5 from flexible-based 0.44 kt TNT case, it can be concluded that a blast magnitude of 0.44 kt TNT (approximately 1100 tons of Ammonium Nitrate) best captures reality and silos' displacement. It should be noted that a displacement of 27.7 cm was obtained in silos 4 and 5 for the 0.44 kt TNT-fixed-based case. This estimation is close to Rigby et al. [6], Stennett et al. [9] and Pasman et al. [10] results. Therefore, the novelty of this study lies in the accurate estimation of the blast magnitude by comparing the FE results, that were based on the real plans and silos' project data, to the 3D scan results while considering SSFI effect. Fig. 16 shows the damage in compression and tension for the 0.44 kt TNT flexible and fixed-based cases. Moreover, Fig. 17 presents the cumulative surface damage rate curves. These curves indicate the state of damage of the silos' elements. On the ordinate is the percentage of damaged surface having undergone the amount of damage indicated while on the abscissa is the damage indicator (1 refers to completely damaged elements/surfaces).

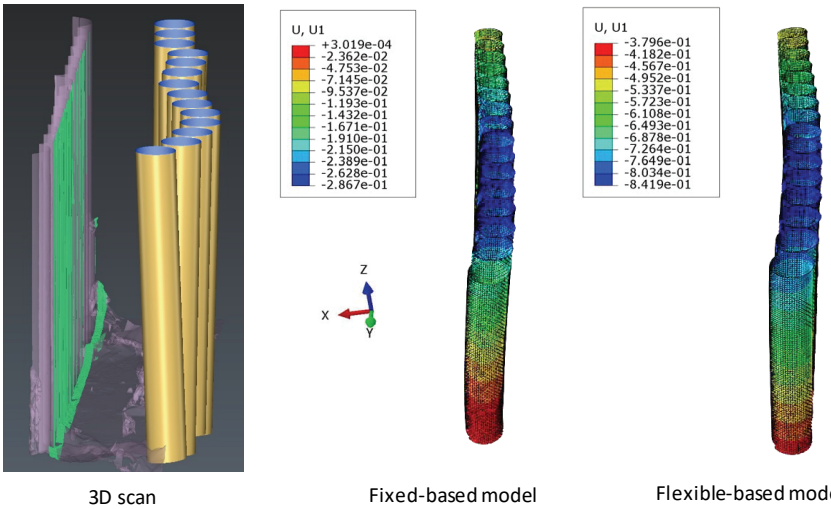

Fig. 14. Displacement of the silos in the direction of the blast (in m) – 0.44 kt TNT FE model case

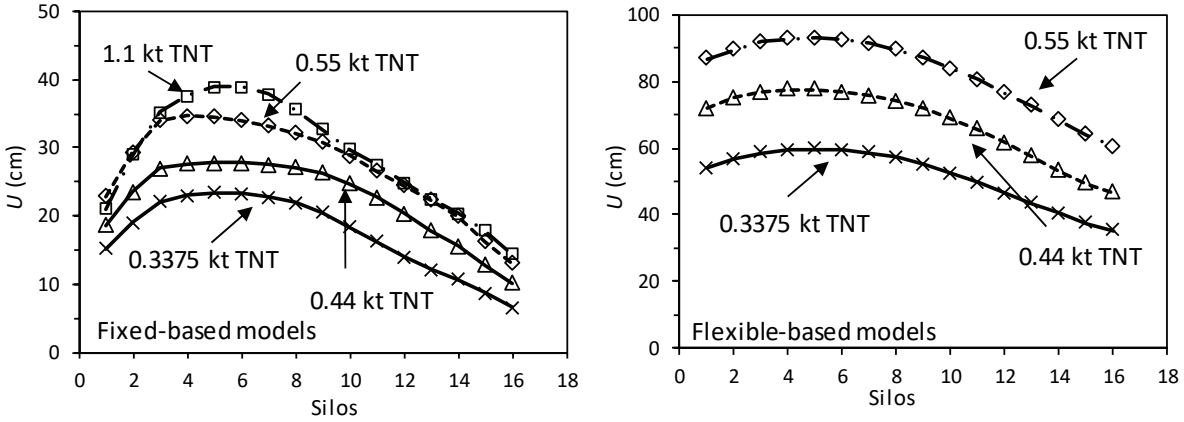

Fig. 15. Permanent displacement at the head of the silos for different blast magnitudes

Table 3. Permanent displacement in the direction of the blast (cm)-Silos 4 and 5

Silos	3D scan		Flexible-based models					
			0.3375 kt TNT		0.44 kt TNT		0.55 kt TNT	
	head	bottom	head	bottom	head	bottom	head	bottom
4	70	55	59.5	29.8	77.4	35.8	92.5	43.5
5	70	50	59.7	29.8	77.5	35.8	93	43.5

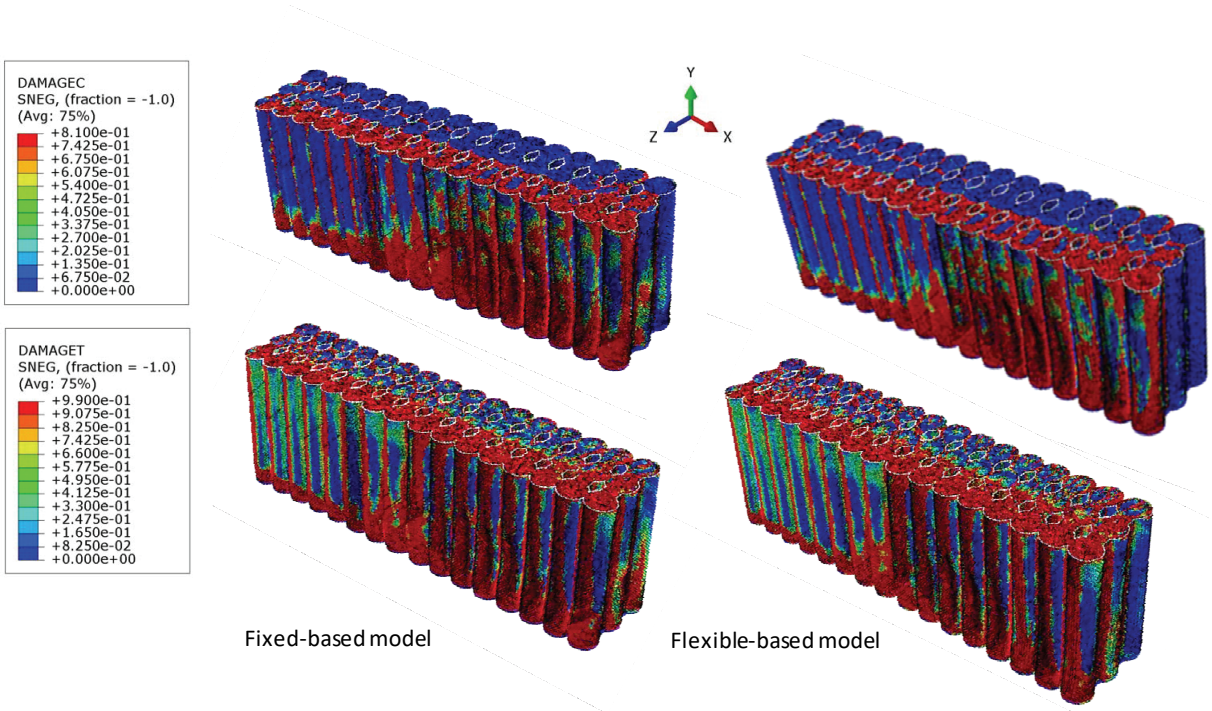

Fig. 16. Damage in compression and tension of 0.44 kt TNT (FE results) (Damage variables range from 0 (no damage) to 1 (destruction))

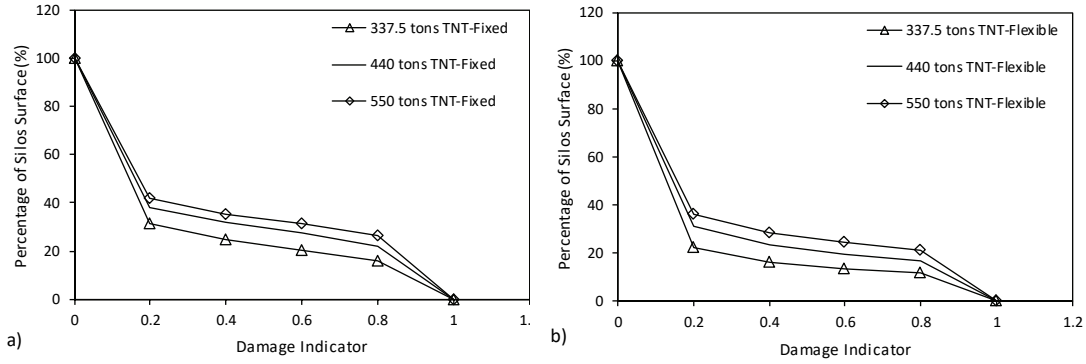

Fig. 17. The cumulative surface damage rate curve of a) fixed and b) flexible-based cases

Hence, fixed and flexible-based FE models were simulated in order to estimate the contribution of the soil medium and foundation to the silos' response due to blast loading. The relative displacement (head with respect to bottom) was obtained in fixed-based models while the flexible-based models allowed a closer and better estimation of silos' displacement at the head and bottom due to the SSFI effects. Therefore, to identify the role of the SSFI effect in the blast, the relative displacement as well as the amount of energies released from the fixed and flexible simulated cases were considered. The results show that the ratio of relative displacement (head to bottom) of flexible to fixed-bases cases is equal to 1.29, 1.50 and 1.42 for 0.3375, 0.44 and 0.55 kt TNT cases respectively (Fig. 15 and Table 4). The FE results show that for the 0.44 kt TNT estimated simulated case, the dissipated energy (the wasted energy outside the model) is 16% lower in flexible than in fixed-based modeled cases. Similarly, the strain energy (the energy stored in the model under the blast loading) is 11% lower in flexible than in fixed-based modeled cases. However, the kinetic (the energy a body possesses by being in motion) and the total energy (the sum of all potential energies in the system) released from the models are 1.87% and 6.28% greater in flexible than in fixed-based cases. While the internal energy and external work are almost the same in both models. As a result, for the 0.44 kt TNT estimated blast magnitude case, the 50% increase in silos' deformation in the direction of the explosion caused 6.28% of the released energy to be transferred into useful energy. That is why the flexible-based case exhibited 16% less wasted energy while storing 11% more strain energy than the fixed-based case. Therefore, even though flexible-based cases possessed higher silos' relative displacement and total energy, the soil and foundation played a positive role in the explosion by storing more while dissipating less amount of energies. It should be noted that the percentage of total energy released by the 0.44 kt TNT is only 1% higher in flexible than in fixed-based models and accounts for 0.06% of the total energy released by the explosion. This value was calculated by dividing the external work exhibited by the FE model to the

explosion released energy, equivalent to 1.84×10^{12} J (every 1 ton of TNT releases 4.184×10^{9} J). As a result, the 3D scan and FE results indicate that the obtained 20 to 30 cm silos' displacements made them out of tolerance with respect to all design codes such as Eurocode [39,43]. As for the foundation, as shown in Fig. 18, the pile cap as well as the head of the driven piles displace on average 35 cm in the direction of the explosion for the 0.44 kt TNT case. This value exceeds the allowable limits in all design codes. As a result, the piles' head were deformed beyond their elastic limit and thus, the pile foundation cannot be reused to build new silos at the same place.

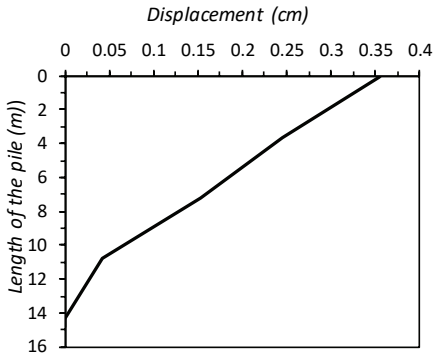

Fig. 18. Displacement of the driven pile-0.44 kt TNT (FE results)

Table 4. Comparing the relative displacement in the direction of the blast (cm)-Silos 4 and 5

Silos	Flexible-based models			Fixed-based models		
	Relative displacement			Displacement at the head		
	0.375 kt TNT	0.44 kt TNT	0.55 kt TNT	0.375 kt TNT	0.44 kt TNT	0.55 kt TNT
4	29.7	41.63	49.08	23	27.7	34.6
5	29.9	41.69	49.51	23.3	27.8	34.5

5.2. Silos' structural response against the filling of the silos

It is important to note that at the time of explosion, the silos were not totally filled with grains (wheat and corn). Therefore, the grains increased the mass of the thin concrete shell silos. As such, the effect of the silos' structural response against the filling of the silos become relevant parameter that may affect the behavior and damage of the silos. To investigate this effect at the time of the event, the absence and presence of grains were first simulated for the fixed-based case scenario for different blast magnitudes. Then, for the estimated blast magnitude: 0.44 kt TNT, the absence and presence of grains were studied for the fixed and flexible cases. The silos' deformations were extracted from the FE models and plotted in Fig. 19. The first and second row of silos, containing most of the grains are completely damaged. The third row of silos was partially filled with grains

with some empty silos (Silos 7, 8, 12, 13, 14 & 15). This led the grains to separate from the concrete silos in the first two rows. As shown in this figure, the silos' deformations were slightly affected by the extra mass of the grains. In fact, the displacement in the direction of the explosion at the head of the silos is almost the same for the different blast magnitudes. This result was also obtained for the 0.44 kt TNT flexible modeled cases. Noting that different types of energies are almost the same for the 0.44 kt TNT flexible modeled cases. Therefore, even though the mass of the silos differ between the two cases and the grains apply pressure on the silos in an order of –147 to 15.5 kPa; nevertheless, the tension on the silos' walls vary 1 to 2% between the 2 studied cases. The tension varies between 2.497 to –37.26 MPs and between 2.28 and –37.675 MPa for the cases with and without grains respectively. That is why the presence of grains on August 4, 2020 had very small influence on the silos' displacement and damage amount.

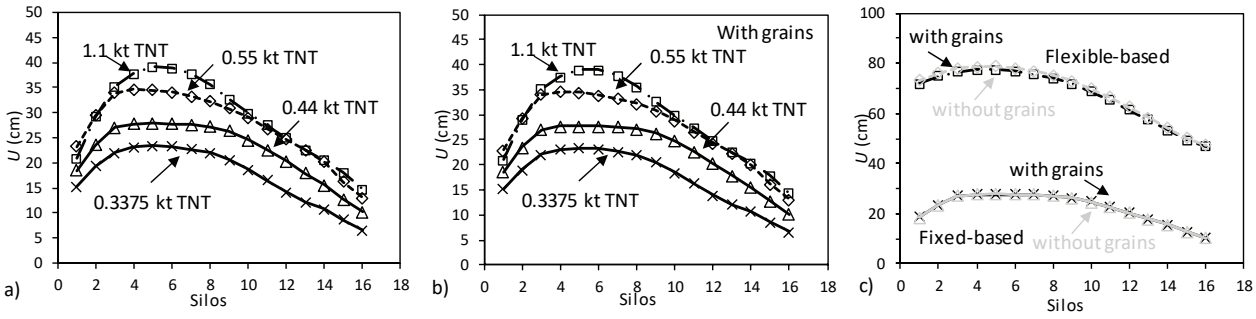

Fig. 19. Permanent displacement at the head of the silos: a and b) for different blast powers and c) for 0.44 kt TNT cases-the silos' structural response against the filling of the silos

6. Conclusions

Using three-dimensional laser scanner and finite element simulations, the Beirut port silos' damage followed by August 4, 2020 explosion was investigated while considering SSFI effect. The 3D scan was performed by Saint Joseph University of Beirut "the school of engineering ESIB" in collaboration with "Amann" engineering, while the numerical simulations were performed using Abaqus explicit. The 3D fixed and flexible-based models, based on the real-plans and project data and consisting of the concrete silos, the soil medium, the pile cap as well as the pile foundation, were hit by the blast loading. The numerical modelling results: the silos displacements in the direction of the blast as well as the amount of silos' damage (in tension, in compression and the cumulative surface damage) were compared to the 3D scan results in order to estimate the blast magnitude and to check if the pile foundation can be reused to build new silos at the same place due

to the limited space available at the port of Beirut. In addition, the silos' structural response against the filling of the silos at the time of the explosion was considered.

The 3D scan, performed in two phases using two different equipment: the LEICA BLK360 and the Z+F Imager 5010X equipment, used 752 million points of measures in three dimensions using 25 stations in 360° panorama infrared images. The scan results showed the silos' state of damage after the explosion. The first two rows of Beirut port silos were destroyed while their bases are still visible filled by wheat and corn. On the other hand, the third row of silos except the last two silos, remained intact. Nevertheless, they tilted from 0 to 70 cm at the head and from 0 to 55 cm at the bottom with respect to the first silo. Therefore, they tilted around 20 to 30 cm (relative deformation head to bottom) in the direction of the blast.

A blast magnitude of 0.44 kt TNT (approximately 1100 tons of Ammonium Nitrate) was found to best captures reality and silos' displacement. The results indicated that SSFI played a positive role in this blast by storing more while dissipating less amount of energies. The percentage of total energy released by the 0.44 kt TNT is only 1% higher in flexible than in fixed-based models and accounts for 0.06% of the total energy released by the explosion. As for the silos' structural response against the filling of the silos, the results showed that the displacement of the silos in the direction of the explosion is almost the same for fixed and flexible-based models and for different blast magnitudes. Hence, the results showed that the presence of grains on August 4, 2020 has no influence on the silos' displacement and damage amount. Finally, the results indicated that the pile foundation cannot be reused to build news silos; the displacements of the silos and the piles are greater than the allowable displacements set by design codes.

Acknowledgments:

The authors would like to acknowledge the support of the Lebanese authorities, Lebanese Army as well as the assistant of Prof. Salah Sadek from the American University of Beirut, Saint Joseph University-ASCE student chapter (ESIB), Francois Karam for the drone pictures, Miguel Bandera for the 3D modelling and photogrammetry and M. Christoph Fröhlich, Chris Held de Zoller and Fröhlich GmbH ("Z+F") for their logistics and financial efforts for using the the Z+F Imager 5010X scanner (Zoller & Fröhlich).

References

[1] How a Massive Bomb Came Together in Beirut's Port, The New York Times, https://www.nytimes.com/interactive/2020/09/09/world/middleeast/beirut-explosion, 2020.

[2] How powerful was the Beirut blast Reuters Graphics, https://graphics.reuters.com/LEBANON-SECURITY/BLAST/yzdpxnmqbpx/, 2020.
[3] A. Bauer, A. King and R. Heater, The detonation properties of ammonium nitrate perils, Department of Mining and Engineering, Queens University, Canada, 1978.
[4] A. King, A. Bauer and R. Heater, The explosion hazards of ammonium nitrate and ammonium nitrate based fertilizer compositions, Department of Mining and Engineering, Queen's University report to the Canadian Fertilizer Institute and Contributing Bodies, Canada, 1982.
[5] DIRECTIVE 2012/18/EU, The control of major-accident hazards involving dangerous substances, 406 amending and subsequently repealing Council Directive 96/82/EC, 2012.
[6] S. E. Rigby, T. J. Lodge, S. Alotaibi, A. D. Barr, S. D. Clarke, G. S. Langdon and A. Tyas, "Preliminary yield estimation of the 2020 Beirut explosion using video footage from social media", *Shock Waves*, 2020. https://doi.org/10.1007/ s00193-020-00970-z
[7] J. Diaz, "Explosion analysis from images: Trinity and Beirut", in: arXiv preprint arXiv:2009.05674, 2020.
[8] C. Aouad, W. Chemissany, P. Mazzali, Y. Temsah and A. Jahami, "Beirut explosion: Energy yield from the fireball time evolution in the first 230 milliseconds", in: arXiv preprint arXiv:2010.13537, 2020.
[9] C. Stennett, S. Gaulter and J. Akhavan, "An estimate of the TNT-equivalent net explosive quantity (NEQ) of the Beirut Port explosion using publicly-available tools and data", *Journal of Propellants, Explosives, Pyrotechnics* vol. 45, pp. 1675–1679, 2020. https://doi.org/10.1002/prep.202000227
[10] H. Pasman, C. Fouchier, S. Park, N. Quddus and D. Laboureur, "Beirut ammonium nitrate explosion: Are not we really learning anything", *Journal of Process Safety,* vol. 39, p. 12203, 2020. https://doi.org/10.1002/prs.12203
[11] G. Valsamos, M. Larcher and F. Casadei, "Beirut explosion 2020: A case study for a large-scale urban blast simulation", *Journal of Safety Science,* vol. 137, pp. 105190, 2021. https://doi.org/10.1016/j.ssci.2021.105190
[12] M 3.3 Explosion – 1 km ENE of Beirut, Lebanon, USGS, https://earthquake.usgs.gov/earthquakes/eventpage/us6000b9bx/executive, 2020.
[13] M. Rayhani and M. El Naggar, "Numerical modeling of seismic response of rigid foundation on soft soil", *International Journal of Geomechics,* vol. 8, pp. 336–346, 2008. https://doi.org/10.1061/(ASCE)1532-3641(2008)8:6(336)
[14] A. Shehata, M. Ahmed and T. Alazrak, "Evaluation of soil-foundation-structure interaction effects on seismic response demands of multi-story MRF buildings on raft foundations", *International Journal of Advanced Structural Engineering,* vol. 7, pp. 11–30, 2015. https://doi.org/10.1007/s40091-014-0078-x
[15] J. Rusek , L. Słowik , K. Firek and M. Pitas, "Determining the dynamic resistance of existing steel industrial hall structures for areas with different seismic activity", *Archives of civil engineering,* LXVI vol. 4, pp. 525–542, 2020. http://dx.doi.org/10.24425/ace.2020.135235
[16] D. Mendez, Stunned Salvador suffers second deadly quake in a month, The BG News, http://media.www.bgnews.com/media/storage/paper883/news/2001/02/14/World/Stunned.Salvador. Suffers Second Deadly Quake In A Month-1283510.shtm, 2001 (accessed Jan. 22, 2008).
[17] K. Patel , A. Goswami and S. Adhikary, "Response characterization of highway bridge piers subjected to blast loading"*, Structural Concrete*, vol. 21, no. 6, pp. 2377–2395, 2020. https://doi.org/10.1002/suco.201900286
[18] M. Ismail, Y. Ibrahim, M. Nabil and M.M. Ismail, "Response of a 3-D reinforced concrete structure to blast loading", *International Journal of Advanced Applied Sciences,* vol. 4, no. 10, pp. 46–53, 2017. https://doi.org/10.21833/ijaas.2017.010.008
[19] F. Fu, "Dynamic response and robustness of tall buildings under blast loading", *Journal of Construction and Steel Research,* vol. 80, pp. 299–307, 2013. https://doi.org/10.1016/j.jcsr.2012.10.001
[20] R. Mudragada and S. Mishra, "Effect of blast loading and resulting progressive failure of a cable-stayed bridge". *SN Applied Sciences,* vol. 3, p. 322, 2021. https://doi.org/10.1007/s42452-021-04145-y
[21] C. Zhao, Y. Liu , P. Wang, M. Jiang, J. Zhou, X. Kong, Y. Chen and F. Jin, "Wrapping and anchoring effects on CFRP strengthened reinforced concrete arches subjected to blast loads", *Structural Concrete*, 2020. https://doi.org/10.1002/suco.202000394
[22] W. Wang, R. Liu and B. Wu, "Analysis of a bridge collapsed by an accidental blast loads", *Engineering Failure Analysis,* vol. 36, pp. 353–361, 2014. https://doi.org/10.1016/j.engfailanal.2013.10.022
[23] D. Dunkman, A. Yousef, P. Karve and E. Williamson, Blast performance of prestressed concrete panels, Proc. 2009 Structures Congress, "Don't Mess with Structural Engineers: Expanding Our Role", Austin, Texas, pp. 1297–1306, 2009.
[24] W. Raphael, R. Faddoul, R. Feghaly and A. Chateauneuf, "Analysis of Roissy airport Terminal 2E collapse using deterministic and reliability assessments", *Engineering Failure Analysis*, vol. 20, pp. 1–8, 2012. https://doi.org/10.1016/j.engfailanal.2011.10.001
[25] A. Edalati and H. Tahghighi, "Investigating the performance of isolation systems in improving the seismic behavior of urban bridges. a case study on the Hesarak bridge", *Archives of civil engineering* LXV vol. 4, pp. 155–175, 2019. http://doi.org/10.7428/acc-2019-0052

[26] R. Faddoul, W. Raphael, A.H. Soubra and A. Chateauneuf, "Incorporating Bayesian networks in markov decision processes", *Journal of Infrastructure System,* vol. 19, no. 4, pp. 415–424, 2013. https://doi.org/10.1061/(ASCE)IS.1943-555X.0000134
[27] W. Raphael, E. Zgheib and A. Chateauneuf, "Experimental investigations and sensitivity analysis to explain the large creep of concrete deformations in the bridge of Cheviré", *Case Studies in Construction Materials,* vol. 9, 2018. https://doi.org/10.1016/j.cscm.2018.e00176
[28] W. Raphael, R. Faddoul, F. Geara and A. Chateauneuf, "Improvements to the Eurocode 2 shrinkage model for concrete using a large experimental database", *Structural Concrete*, vol. 13, pp. 174–181, 2012. https://doi.org/10.1002/suco.201100029
[29] K. Kawashima, Y. Takahashi, H. Ge, Z. Wu and J. Zhang, "Reconnaissance report on damage of bridges in 2008 Wenchuan, China, earthquake", *Journal of Earthquake Engineering,* vol. 13, pp. 956–998, 2009. https://doi.org/10.1080/13632460902859169
[30] Beirut silos at heart of debate about remembering port blast, AP news, https://apnews.com/article/international-news-beirut-lebanon-3aec16ceeebca5b6b2b132aed3cd49d8, 2020 (accessed December 10, 2020).
[31] Lebanon navigates food challenge with no grain silo and few stocks, TBS news, https://tbsnews.net/world/global-economy/lebanon-navigates-food-challenge-no-grain-silo-and-few-stocks-116467, 2020 (accessed August 7, 2020).
[32] H.W. Stephens, The Texas City Disaster 1947, University of Texas Press, Texas, USA, 1997.
[33] S. Mannan, Lees' Loss Prevention in the Process Industries. Hazard Identification, Assessment 396 and Control, Elsevier, Third Ed., Oxford, United Kingdom, 2005.
[34] R.J. Mainiero and J.H. Rowland, A review of recent accidents involving explosives transport, National Institute for Occupational Safety and Health (NIOSH), Pittsburgh Research Laboratory, 2007.
[35] REPORT 2013-02-I-TX , U.S. chemical safety and hazard investigation board, Investigation report, 400 West fertilizer company fire and explosion, 2016.
[36] M. Bandera, Beirut port silos scan reconstruction ï 3D model, Silos Expertise Group, Lebanon Ministry of Commerce, 2021. https://sketchfab.com/models/75059e566100492996630bd3c800d951/embed
[37] Abaqus [Computer Software]. Simulia, Inc.
[38] M. E. Hafezolghorani, F. Hijazi and R. Vaghei, "Simplified damage plasticity model for concrete*", Journal of Structural Engineering,* vol. 27, 2017. https://doi: 10.2749/101686616X1081
[39] Eurocode 4, *Actions on structures*, EN 1991-4, 2006.
[40] The Beirut Port Explosion, Forensic Architecture, https://forensic417 architecture.org/investigation/beirut-port-explosion, 2020 (accessed 16 November 2020).
[41] T. Krauthammer, Modern Protective Structures, CRC Press, Taylor & Francis Group, 2008.
[42] HSE, Safety Report Assessment Guide: Chemical warehouses – Hazards, Health and Safety Executive, United Kingdom, 2012.
[43] Eurocode 2, *Design of concrete structures*, EN 1992-1-1, 2004.

Received: 2021-03-13, Revised: 2021-04-27